(one in the $^1A_{1g}$ and the other in the $^1B_{2u}$), an excimer is trapped and maintained within the cage. At higher temperatures, the thermal kinetic energy overcomes this cagelike environment resulting in the dissociation of excimers to generate $^1B_{2u}$ and $^1A_{1g}$ monomers. The fluorescence lifetime in low-concentration samples of the above solvents at low temperature is within experimental error of that of the isolated molecule in the gas phase; this lifetime varies little over the entire temperature range of these liquids. The implication here is that the small thermal kinetic energy available at low temperature (80-220 K) does not quench the $^1B_{2u}$ state of benzene even though the collision frequency is extremely high. Caging effects of the solvent, that is some structural stability of the solute–solvent shell system, are consistent with such

evidence. The observation of a high rate of relaxation for benzene in room-temperature liquids is most likely due to a thermal nonradiative quenching pathway ~ 2500 cm^{-1} above the zero-point level of the $^1B_{2u}$ state.

The different $^1B_{2u}$ lifetime behavior found for the C_3H_6 and 1-C_4H_8 solvent systems is tentatively attributed to $^1B_{2u}$/triplet-state solvent collisional energy transfer. The possibility of impurity quenching for these solvents is argued to be less likely.

Spectroscopic Studies of Pyrazine in Cryogenic Solutions

J. Lee, F. Li, and E. R. Bernstein*

Department of Chemistry, Colorado State University, Fort Collins, Colorado 80523 (Received: June 28, 1982; In Final Form: August 30, 1982)

The first excited singlet ($^1B_{3u}$) and triplet ($^3B_{3u}$) states of pyrazine are studied in the cryogenic liquids CH_4, C_2H_6, C_3H_8, C_4H_{10}, C_2H_4, C_3H_6, and 1-C_4H_8. The reported data include $^1B_{3u} \leftrightarrow {}^1A_{1g}$ absorption, fluorescence, and lifetimes and $^3B_{3u} \rightarrow {}^1A_{1g}$ phosphorescence and lifetimes as a function of temperature and concentration. From the behavior of the $^1B_{3u} \leftrightarrow {}^1A_{1g}$ system it is concluded that hydrogen bonding is an important feature of the intermolecular potential in these solutions. The lifetime of the singlet state is quite short with an upper limit of ~ 5 ns. The $^3B_{3u} \rightarrow {}^1A_{1g}$ phosphorescence has a measured 4-ms lifetime at 90 K which is consistent with an impurity quenching mechanism and impurity concentration of 0.01 ppm. It has been possible to separate out radiative, nonradiative, and impurity quenching rate constants in these systems for the $^3B_{3u}$ state of pyrazine. An activation energy for the temperature-dependent radiationless process of ~ 2 kcal/mol is regarded as the hydrogen-bonding energy between solvent and pyrazine (N$\cdots$HC) in the excited $^3B_{3u}$ state.

I. Introduction

Relaxation times and absorption and emission spectra have been demonstrated to yield important new information concerning the properties and structure of cryogenic liquids.[1] The observed Franck–Condon shifts between the absorption and emission origins and temperature-dependent low-energy tails of the main features in the emission spectrum of C_6H_6 and $C_{10}H_8$ systems have provided new insights into the intermolecular interactions between solute and solvent molecules. These effects can be understood on the basis of the known qualitative behavior of the polarizabilities of aromatic systems. The fluorescence lifetimes of these systems have been shown to be roughly the same as those observed in very dilute gases (i.e. ~ 150 ns for C_6D_6 and ~ 250 ns for $C_{10}H_8$). The phosphoresence of these molecules has yet to be observed in cryogenic liquids, most likely due to a lack of solvent purity. (For a 1-s lifetime to be realized, an O_2-like quencher must not be present at concentrations greater than 10^{-5} ppm.)

Unlike the previously mentioned systems, the pyrazine molecule undergoes $n\pi^*$ transitions upon excitation to its

first excited singlet ($^1B_{3u}$) and first excited triplet ($^3B_{3u}$) states. Consequently, the excited-state pyrazine system represents a different possible probe of the intermolecular interactions, structure, and dynamics of cryogenic solutions. The spectroscopic properties of pyrazine are now well established for gas[2,3] and solid[4,5] phases. A careful comparison and correlation of the spectroscopic data for pyrazine in all three states of matter can now be made. The results of such studies discussed in this report indicate that hydrogen bonding (N$\cdots$HC) and diffusion-controlled impurity quenching processes play an important role in cryogenic solutions (CH_4, C_2H_6, C_3H_8, C_4H_{10}, C_2H_4, C_3H_6, and 1-C_4H_8). The hydrogen-bonding strength, phosphorescence lifetime for pyrazine as a function of temperature, and a limit to the impurity concentration in these solvents can be measured.

II. Experimental Section

The general preparation and purification procedures for the solvents and solute have been discussed in the previous reports.[1] So that the phosphorescence lifetime of the long-lived triplet state of pyrazine can be measured, highly

(1) (a) Li, J. Lee, and E. R. Bernstein, *J. Phys. Chem.*, accepted for publication. (b) M. Schauer, J. Lee, and E. R. Bernstein, *J. Chem. Phys.*, **76**, 2773 (1982). (c) E. R. Bernstein and J. Lee, *Ibid.*, **74**, 3159 (1981). (d) J. Lee, F. Li, and E. R. Bernstein, *J. Phys. Chem.*, accepted for publication.

(2) Y. Udagawa and M. Ito, *Chem. Phys.*, **46**, 237 (1980).
(3) A. Frad, F. Lahmani, A. Tramer, and C. Tric, *J. Chem. Phys.*, **60**, 4419 (1974).
(4) B. J. Cohen and L. Goodman, *J. Chem. Phys.*, **46**, 713 (1967).
(5) S. L. Madej, G. D. Gillispie, and E. C. Lim, *Chem. Phys.*, **32**, 1 (1978).
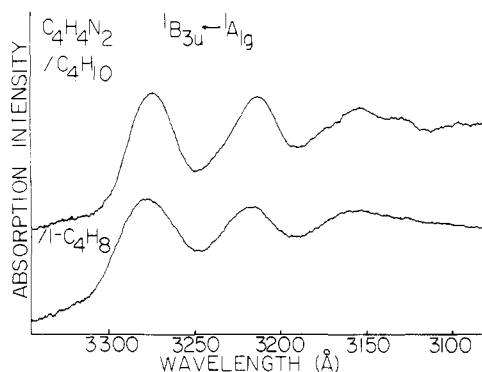
Figure 1. $^1B_{3u} \leftarrow {}^1A_{1g}$ absorption spectrum of ~18 ppm of pyrazine in C_4H_{10} at 180 K and 1-C_4H_8 at 100 K. Both spectra are temperature independent.

TABLE I: Pyrazine $^1B_{3u} \leftarrow {}^1A_{1g}$ Absorption 0_0^0 Energies and Gas-to-Liquid (G–L) Shifts for Various Solvents

solvents	0_0^0 energy ±20, cm^{-1}	G–L shifts,[a] cm^{-1}
C_2H_6	30 574	-296
C_3H_8	30 558	-312
C_4H_{10}	30 546	-324
C_2H_4	30 640	-230
C_3H_6	30 546	-324
1-C_4H_8	30 511	-359

[a] Gas-phase $0_0^0 = 30870$ cm^{-1}.[2]

purified solvents are essential. In addition to careful vacuum distillation through 4A molecular sieve and activated charcoal and freeze–thaw pumping cycles in a grease-free vacuum system, vacuum distillation through RIDOX (Fisher) oxygen scavenger is also employed in an attempt to ensure oxygen-free solvents.

Detailed instrumental setups and procedures for absorption and fluorescence measurements are also presented in the previous papers from this laboratory on cryogenic solutions. The phosphorescence signals are monitored by gated photon-counting techniques. The phosphorescence lifetime is measured by setting a 1-m monochromator (2400 grooves/mm) at the emission origin of the triplet state and scanning the gated photon-counting system 1 μs after excitation. The average intensity at each time interval is then fitted to a single exponential decay by an HP9845S computer.

III. Results and Comparison to Other Systems

A. $^1B_{3u} \leftrightarrow {}^1A_{1g}$: *Absorption and Emission.* The transition between the $^1B_{3u}$ and $^1A_{1g}$ states of pyrazine has been recognized as the excitation of an electron from a nonbonding n orbital of the nitrogen atom to the antibonding π^* orbital of the aromatic ring. The absorption and fluorescence spectra have been analyzed in the low-pressure gas.[2] Figure 1 shows the absorption spectra of pyrazine in C_4H_{10} and 1-C_4H_8 solvents. Table I summarizes the 0_0^0 transitions and gas-to-liquid shifts of pyrazine in different solvents. All spectra are red shifted with respect to the gas-phase transition by roughly 300 cm^{-1}. The bandwidth of the $n\pi^*$ vibronic transitions of pyrazine is comparable to the bandwidth of the $\pi\pi^*$ vibronic transitions of benzene and naphthalene in corresponding solvents (200 cm^{-1}). The absorption spectra of pyrazine, like those of the C_6H_6 and $C_{10}H_8$ systems, are independent of temperature in all solvents.

Figure 2 gives the absorption and fluorescence spectra of pyrazine in C_2H_6 at 100 and 180 K. The temperature-dependent 0_0^0 fluorescence energies are plotted in Figure 3 for four different solvents. Two distinct aspects of these
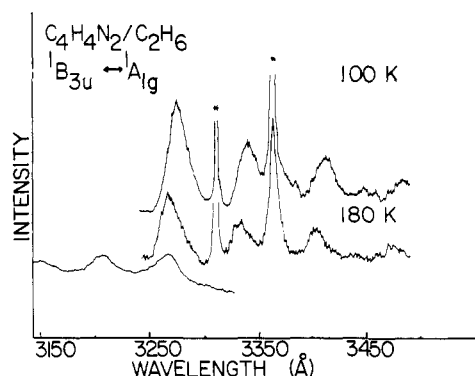

Figure 2. $^1B_{3u} \leftrightarrow {}^1A_{1g}$ absorption and fluorescence spectra for ~16 ppm of pyrazine in C_2H_6 at 100 and 180 K. The absorption spectrum is temperature independent. Peaks markedk with * are Raman scattering of the C_2H_6 solvent. Note the shift in peak positions of the fluorescence features as temperature is changed.
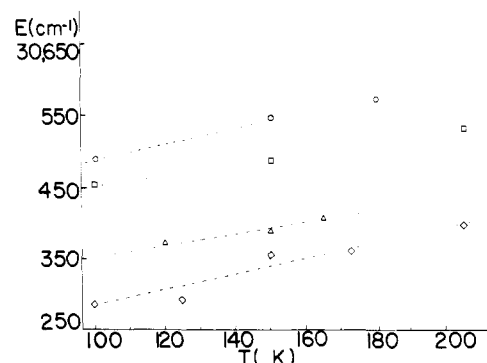

Figure 3. The temperature dependence of the fluorescence 0_0^0 energies in four different solvents: (O) C_2H_6; (Δ) C_2H_4; (□) C_3H_8; (◇) C_3H_6.
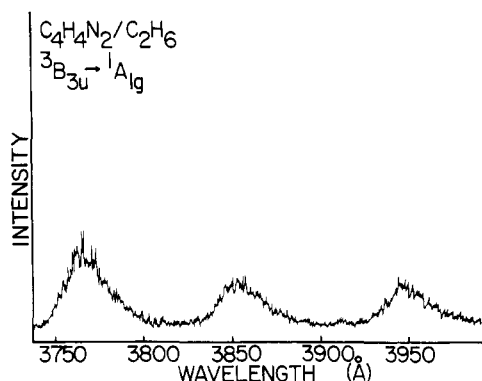

Figure 4. $^3B_{3u} \rightarrow {}^1A_{1g}$ phosphorescence spectrum of ~16 ppm of pyrazine in C_2H_6 at 150 K.

data are apparent after comparison to the $\pi\pi^*$ transitions of benzene and naphthalene. First, the bandwidth is symmetric and without a low-energy tail as temperature is increased. Second, the fluorescence 0_0^0 energy shifts to *higher* energy as temperature is increased.

B. $^3B_{3u} \rightarrow {}^1A_{1g}$: *Emission.* Due to the low oscillator strength of the spin forbidden $^3B_{3u} \leftarrow {}^1A_{1g}$ transition, no direct singlet–triplet absorption is observed in any cryogenic solvent. However, the phosphorescence spectrum, which is enhanced by collision-induced intersystem crossing from the $^1B_{3u}$ state, is observed in CH_4, C_2H_6, C_3H_8, and C_4H_{10} solvents. Figure 4 shows the phosphorescence spectrum of pyrazine in C_2H_6. Table II summarized the 0_0^0 phosphorescence energies and the gas-to-liquid shifts in the above alkane solvents. The bandwidths of the phosphorescence features, which are comparable to the bandwidths for the fluorescence, are symmetric and

TABLE II: Pyrazine $^3B_{3u} \rightarrow {}^1A_{1g}$ Phosphorescence Energies and Gas-to-Liquid (G-L) Shifts for Various Solvents

solvents	0_0^0 energy ± 20, cm^{-1}	G-L shifts,[a] cm^{-1}
CH$_4$	26 603	-58
C$_2$H$_6$	26 540	-5
C$_3$H$_8$	26 506	-39
C$_4$H$_{10}$	26 498	-47

[a] Gas-phase $0_0^0 = 26545$ cm^{-1}.[4]

TABLE III: Observed Triplet-State ($^3B_{3u}$) Lifetimes in C$_2$H$_6$ and C$_3$H$_8$ as a Function of Temperature

	T_1, μs	
T, K	C$_2$H$_6$	C$_3$H$_8$
90	4000	978
100	2813	463
110	1502	231
120	832	141
130	312	70
140	143	43
150	100	22
160	91	17
170	49	

without any temperature dependence. In addition, the phosphorescence features show no evident blue shifts as a function of temperature as observed for the fluorescence.

In the group of alkene solvents (C$_2$H$_4$, C$_3$H$_6$, 1-C$_4$H$_8$), the pyrazine molecule does not phosphoresce. It has been shown that the triplet states of these double bonded solvents (3.4–5.4 eV) overlap the $^1B_{3u}$ and $^3B_{1u}$ states of pyrazine.[6] It is known that the intersystem crossing process is 30 times more efficient for the pathway $^1B_{3u} \rightarrow {}^3B_{1u}$ than it is for the pathway $^1B_{3u} \rightarrow {}^3B_{3u}$.[7] Therefore, it is most likely that these solvents quench the $^3B_{3u}$ phosphorescence by intercepting the intersystem crossing process at the $^3B_{1u}$ state. A similar quenching mechanism has been determined in the gas phase.[8] A further corroboration of this idea comes from the obvious decrease in intensity and lifetime of the $^3B_{3u}$ state phosphorescence in C$_2$H$_6$ as C$_2$H$_4$ is doped into the solution at 9 and 140 ppm. Impurities other than the solvent C$_2$H$_4$ itself are unlikely to quench the triplet state so effectively that the lifetime is reduced to 1 μs. Impurities in C$_2$H$_4$ would have to be present at a concentration of greater than 100 ppm and possess a quenching rate constant of the order of 10^{11} L mol^{-1} s^{-1}.

C. Lifetimes. The fluorescence lifetime of pyrazine in the $^1B_{3u}$ state has been examined in the gas phase[3,7] and in low-temperature glasses.[4] Although the small molecule limit for the long decay time component of the fluorescence has been assigned for pyrazine in the low-pressure gas phase and in collision-free supersonic jet systems,[9] the photophysical behavior for pyrazine in condensed phases seems to correspond to the statistical or large molecule limit.[4] The fluorescence lifetime of pyrazine in condensed phases is in the subnanosecond time regime. Due to the time resolution of our detection instrumentation and laser, an upper limit of 5 ns is observed for a lifetime in all solvents, at all concentrations, and at all temperatures.

The phosphorescence lifetime of the $^3B_{3u}$ state, on the other hand, is relatively long; values of 18.5 ms in the

(6) W. M. Flicker, O. A. Mosher, and A. Kuppermann, *Chem. Phys. Lett.*, **36**, 56 (1975).

(7) K. Kaya, C. L. Chatelain, M. B. Robin, and N. A. Keubler, *J. Am. Chem. Soc.*, **97**, 2153 (1975).

(8) M. Tsukada, *J. Phys. Chem.*, **84**, 827 (1980).

(9) G. ter Horst, D. W. Pratt, and J. Kommandeur, *J. Chem. Phys.*, **74**, 3616 (1981).

TABLE IV: Estimated Impurity Concentration and Diffusion-Controlled Activation Energies in C$_2$H$_6$ and C$_3$H$_8$ [a]

solvents	$K_Q^0[Q]$,[b] s^{-1}	ΔE,[a] cm^{-1}	$[Q]$,[c,d] mol/L
C$_2$H$_6$	2.4×10^4	320	2.4×10^{-7}
C$_3$H$_8$	1.7×10^6	458	1.7×10^{-5}

[a] See text for a more complete discussion and identification of rate constants. [b] Obtained from exponential fit of K_Q. $K_Q = K_Q^0[Q] \exp(-E/k_BT)$. [c] Assuming $K_Q^0 = K_{O_2}^3 \approx 10^{11}$ L/(mol s)) for both solvents.[15] [d] 2.4×10^{-7} mol/L ≈ 0.01 ppm and 1.7×10^{-5} mol/L ≈ 1 ppm.

TABLE V: Pyrazine $^1B_{3u} \leftrightarrow {}^1A_{1g}$ Spectroscopic Properties for Monomer and Aggregate 0_0^0 in C$_3$H$_8$ at 95 K (in cm^{-1})

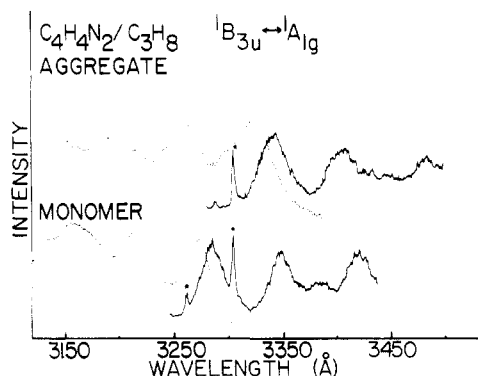|	absorption			fluorescence		
	0_0^0	band-width	G-L shifts[a]	0_0^0	band-width	G-L shift[a]
aggregate	30 100	400	-770	29 950	285	-920
monomer	30 558	225	-312	30 453	225	-417

[a] Gas phase $0_0^0 = 30870$ cm^{-1}.

Figure 5. $^1B_{3u} \leftrightarrow {}^1A_{1g}$ absorption (----) and fluorescence (——) spectra of pyrazine aggregate and monomer in C$_3$H$_8$ at 100 K. Peaks marked with * indicate Raman scattering from the solvent.

low-temperature matrix[5] and 63 μs in the gas phase[3] have been measured. The shorter lifetime in the gas phase is insensitive to pressure from 0.2 to 10 torr and is attributed to a large nonradiative rate ($\sim 10^4$ s^{-1}).[7] In the low-temperature matrix this nonradiative rate is reduced to 37.9 s^{-1} (77 K). In fluid systems, a long-lived triplet state can diffuse to, and be quenched by, impurities. Table III lists the phosphorescence lifetimes of pyrazine as a function of solvent and temperature. Both C$_2$H$_6$ and C$_3$H$_8$ have been carefully and thoroughly degassed and purified as indicated in section II, although impurity free solvents are clearly not attainable. From comparison of the phosphorescence lifetimes, the C$_3$H$_8$ solvent is two orders of magnitude less pure than the CH$_4$ and C$_2$H$_6$ solvents; these results are presented in Table IV.

D. The Aggregate. Aggregation of pyrazine under low-temperature deposition has been verified through absorption spectroscopy and light scattering particle size measurements in cryogenic liquids.[1b] The results indicate that the pyrazine aggregate is crystallike and about 1000 Å in diameter. Figure 5 presents the absorption and fluorescence spectra of the aggregate and monomer in C$_3$H$_8$ at 95 K. Since the aggregate is crystallike, its specrum is not affected by different solvents. Table V outlines the spectroscopic bandwidth and frequency shifts for both species.

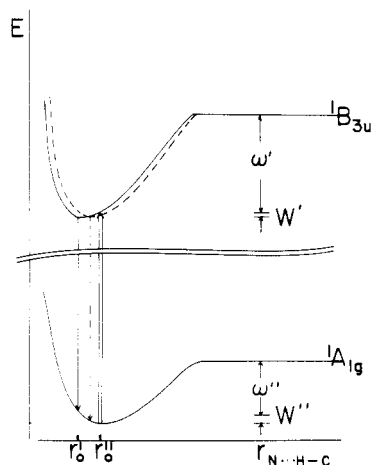Although it would not be expected that any shift between absorption and fluorescence should occur, there is

Figure 6. Intermolecular potentials for the $^1B_{3u}$ and $^1A_{1g}$ states of pyrazine along the hydrogen-bonding coordinate (N···HC): ( ) absorption; (→) emission at low temperature; ( ) emission at high temperature. ω, W, and r_0 are the dispersion energy, the hydrogen-bond energy, and the equilibrium distance for the solute–solvent cage. Primes and double primes imply excited- and ground-state properties, respectively. The zero point energy has been omitted for clarity of presentation.

a 150-cm^{-1} red shift for the emission 0_0^0 with respect to the absorption 0_0^0. This discrepancy may well be associated with defects or traps in the aggregate which collect the excitation energy through energy transfer and subsequently emit from the new configuration.[10]

IV. Discussion

A. Hydrogen Bonding (N···HC). In the liquid state, an intermolecular Franck–Condon shift has been assigned as the cause of the displacement between absorption and emission origins.[1a,11a,12] Due to different charge distributions for the molecular ground and excited states, such shifts reflect the interaction differences of both states. In general, such shifts are dependent on states of the solute molecule, properties of the solvent, and interactions between them. For C_6D_6 and $C_{10}H_8$ solutions[1] the Franck–Condon shifts are discussed in terms of the dispersive forces between solvent and ground- and excited-state solute molecules. In the present systems, however, intermolecular potentials responsible for the Franck–Condon shifts should include hydrogen bonding (N···HC) as well as dispersive forces between solvent and solute systems.

So that the observed Franck–Condon shifts can be related to the intermolecular interactions, it is useful to construct intermolecular potential wells for the ground and excited states of pyrazine in the cryogenic solution. Figure 6 shows schematic plots of the two intermolecular potential wells of the $^1B_{3u}$ and $^1A_{1g}$ states along the localized hydrogen-bonding axis. In this case, the potentials are composed of both hydrogen-bonding interactions (W) and dispersive interactions (ω). The equilibrium solvent–solute separation of the excited state (r_0') is smaller than that of the ground state (r_0'') for the following two reasons: pyrazine polarizes the solvent shell more in its excited state than in its ground state and the n orbital of the N atom shrinks after the excitation of a nonbonding electron to the π^* orbital.[11b] Both of these effects shorten the length of the overall (N···HC) separation, even though the "electronic hydrogen bond" is weaker. Since it is known

that the difference between the dispersive forces in the ground and excited states ($\omega' - \omega''$) does not change with temperature,[1] this contribution to the intermolecular potential can be viewed as a constant, temperature-independent component. The second component, however, hydrogen bonding, is known to change with temperature;[13] that is, hydrogen bonding becomes weaker as temperature increases. The decreased hydrogen bond strength with increased temperature arises in a straightforward manner from the highly asymmetric hydrogen-bonding potential well. Moreover, hydrogen bonding is found to be weaker in the excited state of pyrazine than it is in the ground state ($W' < W''$). It has even been suggested that the hydrogen bond is quite weak in the excited state; it may break and emission may occur from the non-hydrogen-bonded species.[11b] Hence, we expect that the variation of environmental temperature should affect the intermolecular potential of the excited state more than that of the ground state. Figure 6 illustrates the relative position of intermolecular potential wells in both states. Since the excited state is more sensitive to temperature than the ground state, the change in relative positions of the two wells can be viewed as a change in the excited-state well alone. As the temperature increases (dashed line in Figure 6), the excited state becomes less strongly hydrogen bonded and thus less contracted. In other words, as temperature increases the excited-state solvent cage begins to become larger, approaching the size of the ground-state solvent cage. As a consequence of these changes, the fluorescence bands shift to higher energy and retain a symmetric line shape as temperature is increased.

The $^3B_{3u} \rightarrow {}^1A_{1g}$ transition, unlike the $^1B_{3u} \rightarrow {}^1A_{1g}$ transition, shows no temperature-dependent blue shift. The gas-to-liquid shifts of the phosphorescence spectrum ($\sim$30 cm^{-1}) are too small to evidence a significant Franck–Condon effect shift for the $^3B_{3u}$ with respect to the ground state. The intermolecular interactions for the $^1A_{1g}$ and $^3B_{3u}$ states must be nearly identical and both states must have the same sensitivity to changes in the environment. It has been suggested that the $^1B_{3u}$ state has a larger polarizability than the $^3B_{3u}$ state,[13] in agreement with small intermolecular Franck–Condon and gas-to-liquid shift reported herein for the $^3B_{3u}$ state.

B. $^3B_{3u}$ Lifetimes. The decay of the concentration of the triplet state [T], assumed to be related to the decay of the phosphorescence intensity, can be modeled empirically by

$$d[T]/dt = K_1[T] + K_2[T]^2 \qquad (1)$$

K_2 is the second-order bimolecular rate constant and K_1 is the first-order rate constant which includes radiative (K_r), nonradiative (K_{nr}), and impurity quenching (K_Q) rate constants. In general, K_r and K_{nr} are independent of temperature and are treated as constants in this model. K_Q, however, depends on the impurity concentration [Q] and the diffusion constant of the solvent and can be written as

$$K_q = K_q{}^0[Q] \exp[-\Delta E/RT]$$

in which ΔE is the empirical activation energy for solute diffusion to an impurity. In general, $\Delta E \approx \Delta E_\eta$, the diffusion energy of the solvent.

Impurities can thereby play an important if not dominant role in the observed phosphorescence lifetimes for pyrazine in cryogenic liquids. A substantial decrease in

(10) W. R. Moomaw and M. A. El-Sayed, *J. Chem. Phys.*, **48**, 2502 (1968).
(11) (a) G. C. Pimentel, *J. Am. Chem. Soc.*, **79**, 3323 (1957). (b) V. G. Krishna and L. Goodman, *J. Chem. Phys.*, **33**, 381 (1960).
(12) N. S. Bayliss and E. G. McRae, *J. Phys. Chem.*, **58**, 1002 (1954).

(13) G. Neikov and N. Tyretyulkow, *Izv. Khim.*, **12**, 27 (1979).

intensity and lifetime (10^3) is observed for poorly purified solvents.

Triplet-state lifetimes are independent of solute concentration from 2 to 18 ppm, although the solute–solute encounter (diffusion) time at a concentration of 2 ppm is about 10 ns. In addition, the intensity decay of the phosphorescence as a function of time at a given temperature is well fitted by a single exponential decay. Both of these points suggest that the bimolecular self-quenching mechanism is not important for pyrazine in cryogenic liquids; that is, $K_2 = 0$. This result is consistent with the gas-phase data[3,7] for which self-quenching processes are not observed.

The rate equation can then be simplified to

$$-d[T]/dT = K_1[T] \qquad (2)$$

with

$$K_1 = K_{nr} + K_r + K_Q \qquad (3)$$

If K_{nr} and K_r are assumed to be constants over the range of experimental parameters, a plot of $\ln K_1$ vs. $1/T$ should yield ΔE which is expected to be close to ΔE_η. Such a procedure, however, shows that as the solvent purity increases (longer phosphorescence liftimes) ΔE becomes greater than ΔE_η. For example, using the data in Table III we obtain $\Delta E(C_2H_6) = 1.89$ kcal/mol while $\Delta E_\eta(C_2H_6) = 1.0$ kcal/mole and $\Delta E(C_3H_8) = 1.71$ kcal/mol while $\Delta E_\eta(C_3H_8) = 1.31$ kcal/mol. Thus, there must exist another channel competing with the impurity quenching process for the $^3B_{3u}$ state. The best competitor may well be a unimolecular radiationless process that is temperature dependent, as the radiationless rate seems much different in low-temperature glasses than in the gas phase. Hence, the following modification of eq 3 seems appropriate

$$K_1 = K_r + K_{nr}(T) + K_Q(T) \qquad (4)$$

in which both K_{nr} and K_Q are now temperature dependent. So that the nonradiative process could be separated from the quenching process, the following approximations can be made. Since at low temperature $K_Q(T)$ is small in general, and K_r and $K_{nr}(T)$ should be close to the rigid glass 77 K values, we can either assume that K_r and $K_{nr}(T)$ are equal to their 77 K values,[5] $K_{nr}(90 \text{ K}) = K_{nr}(77 \text{ K}) = 37.9$ s^{-1} (model I) or that $K_{nr}(90 \text{ K}) > K_{nr}(77 \text{ K})$ and include (77 K, 37.9 s^{-1}) as an additional data point (model II). $K_Q(90 \text{ K})$ and $K_Q(T)$ can then be obtained from eq 3 and a diffusion-controlled process.[14,15] Based on these two approximate models and the empirical data of $K_1(C_2H_6)$, we can generate a set of temperature-dependent K_{nr} values for each model and fit K_{nr} to an exponential decay. The decay curves for these two models are plotted in Figure 7. Both sets of K_{nr} values are reasonably well fit to the observed phosphorescence lifetimes of pyrazine in C_3H_8, in which now K_Q ($\gg K_{nr}$) plays a dominant role (see Table III). These models predict values of $K_{nr}(300 \text{ K})$ between 10^4 and 10^5 s^{-1}, which is comparable to the observed value for pyrazine at 300 K.[3,7]

The activation energies obtained from these two exponential decay curves are 2.53 kcal/mol (I) and 1.85 kcal/mol (II). The excited-state molecule must overcome a potential barrier of ~ 2 kcal/mol in order to trigger the nonradiative channel in these systems. This barrier can be viewed as a barrier between the hydrogen-bonded and non-hydrogen-bonded excited-state species. As the temperature increases, the excited molecule tends to overcome
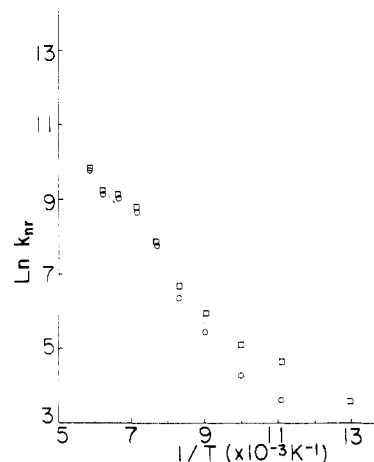

Figure 7. In k_{nr} vs. $1/T$ for the pyrazine $^3B_{3u} \rightarrow {}^1A_{1g}$ system: (O) model I and (□) model II (see text for explanation of these models). These calculations are for pyrazine/C_2H_6 for which impurities do not play an important role in the overall kinetics. The k_{nr} values thus obtained are consistent with the C_3H_8 solvent results for which K_Q impurity quenching is an important factor.

the barrier and relaxes from the non-hydrogen-bonded state with a fast nonradiative rate. In comparison to the general hydrogen-bonding energy (1–7 kcal/mol) the pyrazine (N···HC) system, with potentially two full hydrogen bonds, is relatively weak, as would be expected.

Finally, it is interesting to evaluate the impurity concentrations [Q] and to determine the limiting observable lifetime of the solute phosphorescence due to a residual impurity content in solution. Table IV estimates the concentrations and diffusion-controlled rate constants for the quencher and the diffusion activation energies in these two solvents. Our results for $K_Q^0[Q]$ are of the same order of magnitude as reported by Jackson et al. for room temperature liquids[16] but three orders of magnitude greater than the highly purified naphthalene/3-methylpentane system.[15] Thus, the cutoff maximum observable lifetime we can at present observe is of the order of several milliseconds. For solute molecules of longer triplet state lifetimes, such as benzene and naphthalene, impurity quenching plays a dominant role in triplet-state behavior. If the quencher is oxygen, we may substitute for $K_Q^0 \sim K_0^0 \sim 10^{11}$ L mol^{-1} s^{-1}[17] and obtain [Q] = 2.4 × 10^{-7} mol/L (~ 0.01 pp.n) in the C_2H_6 solvent and [Q] ~ 1 ppm in the C_3H_8 solvent (see Table IV).

V. Conclusions

The differences between the nπ^* transition of pyrazine and the $\pi\pi^*$ transition of naphthalene and benzene used as probes for the structure and dynamics of cryogenic solutions have been discussed in terms of hydrogen bonding (N···HC). Four main points can be made on the basis of the above spectroscopic studies.

1. The addition of hydrogen bonding to the pyrazine-/solvent interaction causes changes of the intermolecular potential as a function of temperature. Thus, the fluorescence spectra are shifted to higher energy as temperature increases.

2. Hydrogen bonding in the excited state tends to reduce the nonradiative processes and results in an activation energy for radiationless decay of roughly 2 kcal/mol for the $^3B_{3u}$ state.

(14) C. A. Parker, "Photoluminescence of Solutions", Elsevier, New York, 1968.
(15) S. C. Tsai and G. W. Robinson, J. Chem. Phys., **49**, 3184 (1968).

(16) G. Jackson and R. Livingston, J. Chem. Phys., **35**, 2183 (1961).
(17) W. R. Ware, J. Phys. Chem., **66**, 455 (1962).

3. Solvent effects on the ground state and the $^3B_{3u}$ state are quite similar.

4. In these cryogenic solvents the triplet-state lifetime is greatly influenced by an impurity quenching process. It has, however, been possible to separate this rate from the intramolecular radiative and nonradiative rates and to arrive at an impurity concentration estimate of 0.01 ppm in C_2H_6. The lifetime measured for the $^3B_{3u} \rightarrow {}^1A_{1g}$ phosphorescence under these conditions is 4 ms which is within a factor of 4 of the longest lifetime measured for this system in a rigid glass.

Fe* Emission Yield and Photoionization of Fe(CO)₅ by Vacuum-Ultraviolet Radiation

David V. Horák[†] and John S. Winn*

Materials and Molecular Research Division, Lawrence Berkeley Laboratory, and Department of Chemistry, University of California, Berkeley, California 94720 (Received: July 23, 1982; In Final Form: August 31, 1982)

A crossed vacuum-UV photon–Fe(CO)₅ molecular beam experiment was used to study the Fe* emission and the Fe(CO)₅ photoionization yields induced by vacuum-UV photons in the 9–21-eV range. Fe emission from quintet spin states was observed, and the total 2000–8500-Å Fe* fluorescence quantum yield was modeled over the 9–14-eV range by a restricted-degrees-of-freedom statistical dissociation model first used to explain Fe fluorescence produced by metastable rare gas collisions. Over this range, absolute cross sections for dissociation into neutrals, dissociation into fluorescing neutrals, and photoionization were determined.

Introduction

Metal carbonyl photochemistry is generally discussed[1] in terms of a single metal–ligand bond rupture or, at most, of two or three such ruptures. In solution phase, or in solid matrices, the chemical consequences of this photochemistry range from simple ligand substitution to photoclustering (or declusterification) to photocatalysis. Virtually all such studies have employed photon sources in the near-UV or visible region, corresponding to photon energies in the range 2–5 eV. Since single metal carbonyl bond energies are typically 1–1.5 eV, one does not expect all metal–ligand bonds to be broken by single-photon absorption in this wavelength range.

In contrast, a number of experiments have demonstrated that all such bonds can be broken if sufficient energy is transferred quickly enough. Thus, metastable atom electronic energy transfer can break all metal–ligand bonds in a single collision;[2] multiple UV photon absorption can similarly produce free atoms (or ions);[3] electron impact dissociation can extensively fragment a metal carbonyl;[4] and, of primary concern in this paper, single vacuum-UV photon absorption can produce free metal atoms from isolated metal carbonyls.[5]

We report here crossed vacuum-UV–molecular beam experiments which elucidate in some detail the fate of iron pentacarbonyl subjected to vacuum-UV photolysis. In brief, we have measured the vacuum-UV absorption cross section, the photoionization quantum yield, and the fluorescence quantum yield for Fe(CO)₅ irradiated throughout the 9.5–14 eV/photon energy range. We also show that our results are consistent with a restricted statistical dissociation model first advanced[2] to explain the metastable atom electronic energy transfer dissociation.

We also confirm the previous reports[5] of spin selectivity in the Fe atom fluorescence spectrum.

Experimental Section

The experimental technique used was that of crossed photon and Fe(CO)₅ molecular beams.[6] Visible fluorescence was monitored in a direction perpendicular to the plane of these beams, and total (mass-undifferentiated) photoion production was monitored by an ion collector as described below.

The vacuum-UV photon source was a cold cathode discharge lamp with a 300 × 6 mm i.d. capillary. The lamp was operated with H₂ to produce the pseudocontinuum emission from ca. 850 to 1650 Å and with He, Ne, and Ar to produce the intense atomic resonance lines at 584 (He), 736 and 744 (Ne), and 1048 and 1067 (Ar) Å. Wavelengths were selected with a 1-m vacuum-UV monochromator operated with slits which passed a 10-Å bandwidth of radiation.

The selected photon beam next entered a chamber containing the Fe(CO)₅ molecular beam. Due to the generally low flux of vacuum-UV radiation available from discharge lamps, this chamber was designed to allow as large a molecular beam flux as possible while maintaining

[†] Present address: IBM General Technology Division, Burlington, VT.

*Address correspondence to this author at his present address: Department of Chemistry, Dartmouth College, Hanover, NH 03755.

(1) G. L. Geoffroy and M. S. Wrighton, "Organometallic Photochemistry", Academic Press, New York, 1979.

(2) D. C. Hartman, W. E. Hollingsworth, and J. S. Winn, *J. Chem. Phys.*, **72**, 833 (1980).

(3) (a) Z. Karny, R. Naaman, and R. N. Zare, *Chem. Phys. Lett.*, **59**, 33 (1978); (b) M. A. Duncan, T. C. Dietz, and R. E. Smalley, *Chem. Phys.*, **44**, 415 (1979); (c) P. C. Engelking, *Chem. Phys. Lett.*, **74**, 207 (1980).

(4) (a) R. E. Winters and R. W. Kiser, *Inorg. Chem.*, **4**, 699 (1964); (b) R. E. Winters and J. H. Collins, *J. Phys. Chem.*, **70**, 2057 (1966).

(5) (a) L. Hellner, J. Masanet, and C. Vermeil, *Nouv. J. Chim.*, **3**, 721 (1979); (b) L. Hellner, J. Masanet, and C. Vermeil, *Chem. Phys. Lett.*, **83**, 474 (1981).

(6) D. V. Horák, Ph.D. Thesis, University of California, Berkeley, CA, 1981 (Lawrence Berkeley Laboratory report LBL-14612).